AIP | Chaos
An Interdisciplinary Journal of Nonlinear Science

# Stalactite basin structure of dynamical systems with transient chaos in an invariant manifold

Vasily Dronov and Edward Ott

Citation: Chaos: An Interdisciplinary Journal of Nonlinear Science **10**, 291 (2000); doi: 10.1063/1.166495
View online: http://dx.doi.org/10.1063/1.166495
View Table of Contents: http://scitation.aip.org/content/aip/journal/chaos/10/2?ver=pdfcov
Published by the AIP Publishing

# Stalactite basin structure of dynamical systems with transient chaos in an invariant manifold

Vasily Dronov[a)] and Edward Ott
*Institute for Plasma Research, University of Maryland, College Park, Maryland 20742*

(Received 1 September 1999; accepted for publication 22 February 2000)

Dynamical systems with invariant manifolds occur in a variety of situations (e.g., identical coupled oscillators, and systems with a symmetry). We consider the case where there is both a nonchaotic attractor (e.g., a periodic orbit) and a nonattracting chaotic set (or chaotic repeller) in the invariant manifold. We consider the character of the basins for the attracting nonchaotic set in the invariant manifold and another attractor not in the invariant manifold. It is found that the boundary separating these basins has an interesting structure: The basin of the attractor not in the invariant manifold is characterized by thin cusp shaped regions (''stalactites'') extending down to touch the nonattracting chaotic set in the invariant manifold. We also develop theoretical scalings applicable to these systems, and compare with numerical experiments. © *2000 American Institute of Physics.* [S1054-1500(00)00502-4]

**Dynamical systems that exhibit chaotic dynamics on an invariant manifold embedded in their state space are of interest in a variety of situations, and examples show that these situations may yield novel dynamical behaviors. One such situation is the case where the chaotic set in the invariant manifold is attracting on average but has within it invariant subsets that are repelling transverse to the invariant manifold. In appropriate circumstances this leads to so-called ''riddling'' of the basin of attraction. In this paper we consider a related but different situation where there is both a nonattracting chaotic set and an attractor which is ''absolutely attracting'' in the invariant manifold. Here, by ''absolutely attracting'' we mean that the attractor is attracting for points in the invariant manifold and contains no invariant subsets that are nonattracting transversely (e.g., the absolutely attracting attractor might be a stable periodic orbit). Thus in the full phase space there is an open neighborhood of the absolutely attracting attractor that is part of its basin of attraction. It is found that in such a case the basin boundary of the attractor in the invariant manifold may be characterized by a thin stalactitelike structure emanating from the nonattracting chaotic set in the invariant manifold. We employ a Fokker–Planck type model which shows that, near the invariant manifold, the state space measure (volume) not in the basin of the attractor on the invariant manifold scales as a power law of the displacement from the invariant manifold. The solution to the Fokker–Planck model for the power law exponent is in a good agreement with numerical tests.**

## I. INTRODUCTION

Recently, physically important examples of dynamical systems that have invariant manifolds embedded in their phase space have been studied, and some important dynamical consequences of this have been revealed. An important class of systems that have invariant manifolds are those that possess an appropriate symmetry. In this case any initial state that has the same symmetry as the system evolves to other states that also respect the symmetry of the system. The set of such symmetric initial states then forms a manifold that is invariant under the dynamics of the system. An example of an invariant manifold not accompanied by a symmetry of the dynamical system is the case of one-way coupling of two identical oscillators, for which the states where the oscillators are synchronized form an invariant manifold.

An invariant manifold (whether induced by symmetry or not) can also have the property that the dynamics restricted to this manifold is chaotic, i.e., initial states in the manifold can be attracted to some chaotic set $A$ in the invariant manifold. Thus $A$ is an attractor for initial conditions in the invariant manifold. Note, however, that $A$ may or may not be an attractor for the full system. Here, by an attractor for the full system we mean that the set $A$ attracts a set of initial conditions of positive Lebesgue measure in the full phase space.[1] In what follows, if we say, without qualification, that $A$ is an attractor, then we mean that it is an attractor for the full system.

Considering the case where $A$ is an attractor, there are typical cases where there is a small set of points in any neighborhood of the invariant manifold that move away from $A$ as the dynamical system evolves. If the global dynamics of the system is such that these repelled orbits are attracted to a set other than $A$, then the basin of attraction of $A$ is *riddled*.[2,3] That is, if $r$ is any point in the basin of $A$, then, for every $\nu$, no matter how small, there is a displacement $\delta, |\delta| < \nu$, such that the point $r+\delta$ is in the basin of another attractor, and the set of such points, $r+\delta, |\delta|<\nu$, has nonzero phase space volume (i.e., positive Lebesgue measure). This presents a basic obstruction to determinism in such systems: If one does an experiment by preparing an initial condition and observes that the resulting orbit goes to $A$, then no matter how great

[a)]Electronic mail: dronov@glue.umd.edu

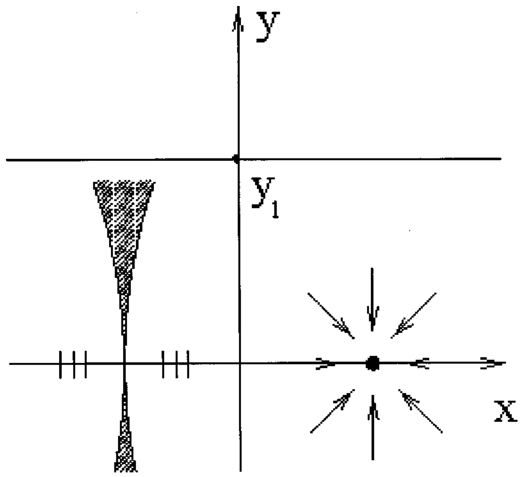


FIG. 1. Schematic of the situation where there is a chaotic repeller (vertical tic marks) and a periodic orbit (closed circle) in the invariant manifold ($y=0$).

one's precision in preparing the initial condition, one cannot be sure that an attempted repeat of the experiment will result in the same outcome.

The unusual properties of riddled basins have received much attention. Recent work[4–7] has investigated the transition to chaotic attractors with riddled basins and the effect of noise and asymmetry on the dynamics of systems with riddled basins. To treat the transition to chaotic attractors with riddled basins, a simple analyzable diffusion model[4] was proposed and scaling relations consistent with numerical simulations were obtained.[5]

The main question addressed in this paper is what happens if, instead of a chaotic attractor embedded in the invariant manifold, there is a chaotic repeller for the initial conditions in the invariant manifold.[8] By a chaotic repeller we mean an invariant set on which the dynamics is chaotic, but which does not attract a positive Lebesgue measure set of initial conditions in the invariant manifold. Typically, such nonattracting chaotic sets manifest themselves as chaotic transients.[9] For the case we consider, an initial condition in the invariant manifold can experience a chaotic transient, after which it is attracted to a periodic orbit in the invariant manifold.

As we shall show, when a chaotic repeller is in the manifold, the basin of the periodic orbit attractor in the invariant manifold is no longer riddled, although it still has unusual properties. This new situation is illustrated schematically in Fig. 1, where we use a two-dimensional $x-y$ representation. In Fig. 1, $y=0$ represents the invariant manifold. The closed circle represents the nonchaotic attractor in the $y=0$ invariant manifold, and the vertical tic marks represent the chaotic repeller in $y=0$. From every point in the chaotic repeller there emanates a cusp-shaped region (a stalactite) of the basin of the attractor in $y\neq 0$. Only one of these cusp-shaped regions is shown in Fig. 1, but we emphasize that such regions exist for all points in the chaotic repeller. Note that since the attractor (the closed circle in Fig. 1) attracts a neighborhood of itself, its basin is not riddled. Nevertheless, there is a remnant of the previously studied riddled behavior in the infinite number of cusps of the $y\neq 0$ attractor emanating from the invariant manifold $y=0$. To characterize this situation we shall be interested in the scaling of the size of the $y\neq 0$ attractor's basin in the region near the invariant manifold $(y=0)$. In particular, we will consider a horizontal line $y=y_1$ (see Fig. 1) and ask what is the Lebesgue measure of $x$ values in this line that are attracted to the $y\neq 0$ attractor. We find that for $y_1$ small this measure, denoted $P_\infty(y_1)$, exhibits a power law scaling, $P_\infty(y)\sim y^\alpha$. To arrive at this result, following Ref. 7, we modify the diffusion model of Ref. 4 previously used for the riddled case to account for the new situation pictured in Fig. 1, and we use it to derive results for the scaling exponent $\alpha$. We claim that these results are universal in the sense that they are valid for the class of dynamical systems of the type considered previously.

In order to check our scaling relations numerically we studied three dynamical systems. The first two are represented by two-dimensional maps. In the first two-dimensional map case the dynamics in the invariant manifold is described by the well-known logistic map, and we will be interested in parameter values in the vicinity of a type-one intermittency transition.[10] In the second two-dimensional map case the logistic map is replaced with a map[11] exhibiting type-three intermittency.[10] The third example is a system of ordinary differential equations (a flow) which is a modification of a previously studied system[3] that describes the motion of a particle in a two-dimensional potential well. As before, we are interested in parameter values near an intermittency transition. Our predicted scaling relations were tested for all three numerical models and reasonably good agreement with the theory was observed.

In a recent paper, Lai and Grebogi[12] consider the same situation that we consider here. A main claim in that paper is that the basin is of a mixed type with the property that, in the vicinity of the saddle, the basin is riddled, while in the region of the attracting periodic orbit in the invariant manifold, the basin is solid (i.e., it consists of open volumes and is not riddled). Such a mixed basin cannot occur, and the basin cannot be riddled anywhere. In general, if a basin is open in any neighborhood $\mathcal{N}$ of the attractor, it must be open everywhere. A simple argument showing this is as follows. Say $p$ is a point in the basin. Evolving $p$ forward, it must eventually approach the attractor. Thus, at some finite time, the orbit from $p$ must eventually enter $\mathcal{N}$, say at point $p'$. The point $p'$ in $\mathcal{N}$ necessarily has an open neighborhood in the basin. Since $p$ iterates to $p'$ in a finite number of iterates, $p$ must also have an open neighborhood in the basin. Hence, in contradiction to the claim of Ref. 12, the basin cannot be riddled anywhere. Lai and Grebogi[12] also attempt to obtain the scaling $P_\infty(y)\sim y^\alpha$. However, they use a crude model for the chaotic transient; in particular, in their model all points in the chaotic transient phase abruptly leave the transient at a fixed time equal to the average transient lifetime. In fact, there is a continuous long-time exponential decay of orbits in the chaotic transient, and it is necessary to include this in the model to obtain the correct scaling and the correct exponent $\alpha$.

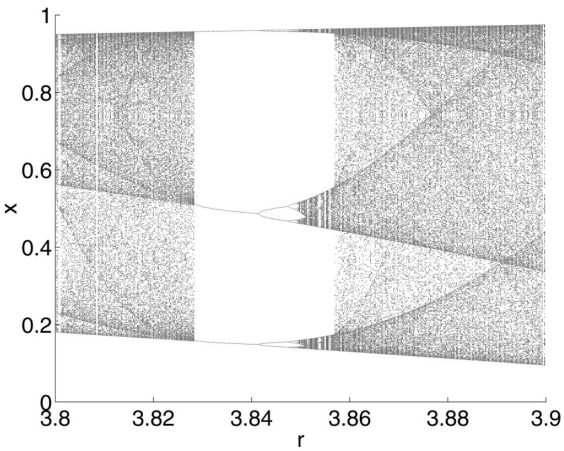


FIG. 2. Period-three window in the bifurcation diagram of the logistic map, $x_{n+1}=rx_n(1-x_n)$.

## II. THE MODEL

Consider a smooth two-dimensional map of the form

$$y_{n+1}=N(x_n, y_n, \epsilon), \tag{1}$$

$$x_{n+1}=M(x_n, r), \tag{2}$$

where $\epsilon$ and $r$ are parameters. Suppose that $N(x,0,\epsilon)=0$ so that there is an invariant manifold at $y=0$. We also assume that $N(\cdot)$ is such that if $|y_n|>y_c$ then all subsequent $y$ iterates are also in $|y|>y_c$; in particular, the orbit never comes back close to the $y=0$ plane. Thus there is another attractor (or attractors) in $|y|>y_c$. Without loss of generality we let $y_c=1$.

Following Ref. 7 we refer to $\epsilon$ as a ''normal'' parameter since it affects the dynamics normal to the $y=0$ invariant manifold, but has no influence on the dynamics in the $y=0$ invariant manifold [the dynamics in $y=0$ is governed by Eq. (2)]. Similarly,[7] we refer to $r$ as a ''non-normal parameter.''

Suppose that for some value of $r$, $M(x,r)$ has a chaotic attractor in $x$ and $\epsilon$ is such that riddling occurs. In this case $y=0$ is an attractor and its Lyapunov exponent, which we denote $h_\perp$ [calculated by taking a differential $y$ variation of Eq. (1)], is negative, $h_\perp<0$. In the riddled case, in any neighborhood of the $y=0$ attractor there are initial conditions that stay in the neighborhood and go to the attractor, as well as other initial conditions that leave the neighborhood of $y=0$, possibly moving to the $|y|>y_c$ attractor. What will happen if we change $r$ in such a way that, for a typical initial condition $x_0$, $M(\cdot)$ generates a chaotic transient instead? [For example, if $M(\cdot)$ is the logistic map we can imagine a change of $r$ such that we enter a periodic window, e.g., the period-three window on the bifurcation diagram of the logistic map; see Fig. 2.] This means that the original chaotic attractor in the invariant plane $y=0$ does not exist any more and typical initial conditions in $y=0$ eventually go to a nonchaotic attractor (e.g., a periodic orbit or a fixed point) as $n\to\infty$. There will still exist, however, an infinite nonattracting set of initial conditions $\{x_0^{\mathrm{inv}}\}$ (representing the ghost of the former chaotic attractor) for which infinitely long chaotic orbits can be generated, and this set has zero Lebesgue measure in $x$.

Let $\langle h_\perp\rangle$ denote the $y$-Lyapunov exponent for a typical orbit on the $y=0$ chaotic invariant set. Here, by ''typical'' we mean with respect to the natural transient measure for the $x$ map. In this case $\langle h_\perp\rangle$ is calculated by sprinkling $N_0$ initial conditions in $y=0$, iterating them for $n$ iterates, discarding those that are near the nonchaotic orbit (say, further than some appropriate distance $l$), calculating the $h_\perp$ exponents over the time interval 0 to $n$ for each orbit not near the nonchaotic orbit at time $n$, and averaging these values. In the limit $N_0\to\infty$, $n\to\infty$, this average is $\langle h_\perp\rangle$, the $y$-Lyapunov exponent, calculated with respect to the natural transient measure for the $x$ map.

We show in the following that the basin of $|y|>y_c$ can be in the form of an infinite set of cusp-shaped regions emanating from the chaotic transient invariant set in the plane $y=0$. We call these cusp-shaped regions stalactites. We show for our examples that the Lebesgue measure in $x$ of these tongues in a $y=y_1$ cross section scales as $y_1^\alpha$, where $\alpha>1$. We also give a theory for determining $\alpha$ and obtain good agreement of the theory with numerical experiments. We note that stalactite boundaries can occur for both $\langle h_\perp\rangle>0$ and $\langle h_\perp\rangle<0$. For stalactites in the case $\langle h_\perp\rangle<0$, however, it is also required that the chaotic saddle (although transversely attracting) have embedded periodic orbits with positive transverse Lyapunov exponents.[12]

## III. DIFFUSION APPROXIMATION

Consider the map (1)–(2) and assume that there is a fixed point attractor $x=x_*$ for almost any initial condition in $y=0$. Also assume that there is a chaotic transient set in $y=0$. The transverse tangent map (evolving differential $y$ displacements from the invariant set $y=0$) is

$$\delta y_{n+1}=N_y(0, x_n)\,\delta y_n,$$

where $N_y(0,x)$ denotes $\partial N/\partial y$ evaluated at $y=0$. For an initial condition $x_0$ precisely on the chaotic transient set, the orbit $x_n$ is typically chaotic. For $x_1$ on the nonchaotic attractor in $y=0$ (i.e., $x=x_*$), we have $|N_y(0,x_n)|<1$. Let $\delta z_n=-\ln|\delta y_n|$. Then the change in $\delta z$ is given by $\delta z_{n+1}=\delta z_n+\Delta_n$, where $\Delta_n=-\ln|N_y(0,x_n)|$. During the chaotic transient $x_n$ is chaotic, and hence $\Delta_n$ varies in a random manner. After the chaotic transient $\Delta_n\cong\ln|N_y(0,x_*)|<0$. We follow Ref. 7 and model this situation as follows: $\Delta_n$ is taken to be of constant magnitude $|\Delta_n|=\Delta$ when the orbit is on the chaotic transient and fluctuations in $\Delta_n$ are modeled by random assignment of its sign $\Delta_n=\pm\Delta$, and we assume that the linearized dynamics is a good approximation to the actual dynamics for finite $y$ in a neighborhood of $y=0$. Thus on any given $\overline{y}\equiv\ln 1/|y|$ an iterate is represented by the step $\overline{y}\to\overline{y}\pm\Delta$, with $\overline{y}=+\infty(\delta y=0)$ corresponding to $y=0$. We consider a Markov chain model described by a semi-infinite chain of states $S_i$, $i=0,1,2,\ldots$ (see Fig. 3). We call the chain $S_i$ the ''chaotic chain.'' The model has three parameters $\beta_+$, $\beta_-$, and $\eta$, which represent the probabilities of the following transitions:

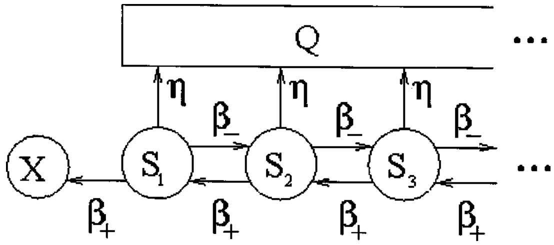


FIG. 3. Markov chain.

$$\beta_+ : S_{i+1} \to S_i \text{ and } S_1 \to X,$$

$$\beta_- : S_i \to S_{i+1},$$

$$\eta : S_i \to Q.$$

The transition $S_{i+1} \to S_i (S_i \to S_{i+1})$ represents a step in $y$ away from (toward) the invariant surface $y=0$, and in $\bar{y}$ it is represented by a step $\bar{y} \to \bar{y} - \Delta (\bar{y} \to \bar{y} + \Delta)$. $X$ represents the condition $|y| > y_c$ for which the orbit goes to an attractor (or attractors) not in $y=0$. After the transition $S_i \to Q (S_1 \to X)$ the orbit is assumed to move uniformly in $x$ (in $y$) toward the periodic attractor in $y=0$ (the attractor in $|y| > y_c$). Once the chaotic chain is exited by transmission to $Q$ or $X$, the chaotic transient is considered to be ended. We identify the transverse Lyapunov exponent with the random walk parameters via $\langle h_\perp \rangle = (\beta_+ - \beta_-)\Delta$. The question now becomes what is the probability of reaching the state $X$ if starting at the state $S_i$. Our purpose in introducing this Markov model is to obtain a result for the scaling of the size of the $y \neq 0$ attractor basin in the region near $y=0$. In particular, consider the horizontal line $y=y_1$. Different initial conditions $x=x_1$ on this line produce orbits, some of which go to the $y=0$ attractor, and some of which go to the $y \neq 0$ attractor. We ask what fraction of the $x$-Lebesgue measure on $y=y_1$ goes to the $y \neq 0$ attractor. Denote this fraction $P_\infty(y_1)$. The above-mentioned Markov model is relevant to this question in the following way. If we choose a point $x_1$ at random on the line $y=y_1$, then the probability that $x_1$ is in the basin of the $y \neq 0$ attractor is $P_\infty(y_1)$. Furthermore, as argued in Ref. 4, while the orbit is chaotic, the orbit generated for random $x_1$ can be regarded as random and as a stochastic process corresponding to a random walk on the $S_i$ chain. However, the orbits following the chaotic transient can leave the $S_i$ chain either by repulsion into the $x$ region where the orbit moves toward the nonchaotic orbit ($x=x_*$ on $y=0$; i.e., $S_i \to Q$) or by repulsion in $y$ into the region $|y| > y_c$ (i.e., $S_1 \to X$). Thus we can identify $P_\infty(y_1)$ with a random walker's probability $p(i)$ of reaching $X$ starting at $i \sim \Delta^{-1} \ln |y_c/y_1|$. In particular, the large $i$ scaling of $p(i)$,

$$p(i) \sim e^{-Ki},$$

and the small $y_1$ scaling of $P_\infty(y_1)$,

$$P_\infty(y_i) \sim |y_1|^\alpha,$$

are connected. Thus we now attempt to estimate $K$ from the Markov model. Once this is accomplished, we will be in a position to use this to conjecture a general result for $\alpha$, which we will compare with numerical experiments in Sec. IV.

For the purposes of obtaining a solution for $p(i)$, we will apply the diffusion approximation, valid for $(\beta_+ - \beta_-)$ small,[4] to the Markov model. Then the basic parameters of the diffusion model are the following:

(1) the average drift along the $S_i$ chain per iterate, $v = \langle \delta \bar{y} \rangle$, where $\delta \bar{y}$ is the increment in $\bar{y}$ in one time step; by definition of the transverse Lyapunov exponent $v = -\langle h_\perp \rangle$;
(2) the diffusion per iterate, $D = \frac{1}{2} \langle (\delta \bar{y} - \langle \bar{y} \rangle)^2 \rangle$, where $\langle \cdots \rangle$ denotes an average over the initial random values of $x_1$;
(3) and an average lifetime of a typical chaotic transient $\tau$.

Let $P(\bar{y}, \bar{y}_1, n)$ be the probability distribution function for $\bar{y}$ (given that $x_1$ is randomly chosen on the horizontal line segment $y=y_1$). Considering $n$ to be approximated by a continuous variable (valid for $n \gg 1$), $P(\bar{y}, \bar{y}_1, n)$ obeys the following drift-diffusion equation:

$$\frac{\partial P}{\partial n} + v \frac{\partial P}{\partial \bar{y}} = -\frac{P}{\tau} + D \frac{\partial^2 P}{\partial \bar{y}^2}. \tag{3}$$

Since we imagine initial conditions all to start at $y=y_1$, we have

$$P(\bar{y}, \bar{y}_1, 0) = \delta(\bar{y} - \bar{y}_1), \bar{y}_1 > 0. \tag{4}$$

Since any orbit which crosses $y = y_c \equiv 1$ ($\bar{y}=0$) is lost to the $y>1$ attractor, we have

$$P(0, \bar{y}_1, n) = 0. \tag{5}$$

As discussed in Ref. 4, for this diffusion approximation to be valid we require two conditions:

(1) Many steps must be taken to reach $y=1$ (corresponding to $\bar{y}=0$), or $\bar{y}_1 \gg 1$.
(2) The drift on each iterate must be small, which means that $|\langle h_\perp \rangle| \ll 1$.

In order to solve Eq. (3) we will introduce the Laplace transform of $P(\bar{y}, \bar{y}_1, n)$ with respect to the continuous time variable $n$,

$$\bar{P}(\bar{y}, \bar{y}_1, s) = \int_0^\infty e^{-sn} P \, dn. \tag{6}$$

Equations (3)–(5) yield

$$D d^2 \bar{P}/d\bar{y}^2 - v \, d\bar{P}/d\bar{y} - (s + 1/\tau)\bar{P} = -\delta(\bar{y} - \bar{y}_1) \tag{7}$$

with the boundary condition $\bar{P}(0, \bar{y}_1, s) = 0$. Solving Eq. (7) is straightforward (see the Appendix).

In Eq. (3), the term $P/\tau$ is the rate at which orbits leave the chaotic transient to move toward the attractor in $y=0$. Thus the probability of going to the attractor in the invariant manifold is

$$P_{y=0} = \frac{1}{\tau} \int_0^\infty \int_0^\infty P(\bar{y}, \bar{y}_1, n) d\bar{y} \, dn \tag{8}$$

and, therefore, the probability of getting attracted to the $y>1$ attractor is

$$P_\infty = 1 - P_{y=0} = 1 - \frac{1}{\tau} \int_0^\infty \int_0^\infty P(\bar{y}, \bar{y}_1, n) d\bar{y} \, dn. \tag{9}$$

Performing the integration we finally get

$$P_\infty = y_1^\alpha, \alpha = [\sqrt{\langle h_\perp\rangle^2 + 4D/\tau} - \langle h_\perp\rangle]/2D. \tag{10}$$

The special case of small $D(D/\langle h_\perp\rangle^2\tau \ll 1)$ yields

$$\alpha \cong \begin{cases} (\langle h_\perp\rangle\tau)^{-1} & \text{for } \langle h_\perp\rangle > 0 \\ -\langle h_\perp\rangle/D & \text{for } \langle h_\perp\rangle < 0 \end{cases}. \tag{11}$$

Note that, as expected, the result for $\langle h_\perp\rangle < 0$ and $\tau \to \infty$ agrees with the result for the exponent in the case of a riddled basin attractor, Ref. 4. In the examples that follow $\langle h_\perp\rangle > 0$.

## IV. NUMERICAL EXPERIMENTS

The universality of the phenomena addressed in this paper implies that very general results may be extracted from simple models that incorporate the essential features responsible for this phenomena. In this spirit we introduce three illustrative examples.

*Example 1*: The first example is the following two-dimensional map:

$$x_{n+1} = M_1(x_n, r) = r x_n(1 - x_n), \tag{12}$$

$$y_{n+1} = N_1(x_n, y_n, \epsilon, \epsilon') = \{1 + \epsilon - \epsilon'[1 - \cos(2\pi x_n)]\} y_n + y_n^3. \tag{13}$$

This system has $N_1(x,0,\epsilon,\epsilon') = 0$. Therefore, $y=0$ is an invariant manifold for the map. The dynamics on this invariant manifold are generated by the logistic map and are independent of the parameters $\epsilon$ and $\epsilon'$. Therefore, the parameters $\epsilon$ and $\epsilon'$ are normal parameters for the system (12) and (13). The value of $\tau$ was chosen to be 3.837, which corresponds to the case of a period-three attractor in the period-three window of the logistic map (see Fig. 2). This implies that typical initial conditions in $0 < x_0 < 1$ and $y_0 = 0$ may generate chaotic transients. The average lifetime $\tau$ of such a transient depends on $r$ and in our case is numerically determined to be $\tau = 21.41$. Note that if $y_n > [\frac{1}{3}(2\epsilon' - \epsilon)]^{1/2}$ then $y_{n+1} > y_n$ and the orbit evolves toward $y = \propto$, which we regard as the attractor not in $y=0$. A numerical approximation to the basins of attraction is shown in Figs. 4(a) and 4(b). To generate this figure we use a $5000 \times 5000$ grid of initial conditions, and we iterate each initial condition until it either reaches $y > [\frac{1}{3}(2\epsilon' - \epsilon)]^{1/2}$ (in which case we plot a closed circle at the location of the initial condition) or else reaches a very small value of $y, y < 2 \times 10^{-5}$. In the latter case we presume that, with high probability, the orbit will go to the $y=0$ attractor. (This is justified by the scaling $P_\infty \sim y^\alpha$). We see in Figs. 4(a) and 4(b) that there are many thin downward pointing black regions. From numerical examination of some of them by magnification of the horizontal scale we find that these thin black regions apparently extend down and touch the invariant set. They are the stalactites referred to in Sec. I. The reason the stalactites appear in Figs. 4(a) and 4(b) to terminate before reaching $y=0$ is that they become so thin as $y$ is decreased that they eventually fail to be resolved by our grid of initial conditions. In our simulations we took $\epsilon' = 0.8$ and varied the value of $\epsilon$. For each value of $\epsilon$ we calculated $\langle h_\perp\rangle$, $D$, $\alpha_{\text{th}}$, and $\alpha_{\text{exp}}$. The data are presented in Table I.

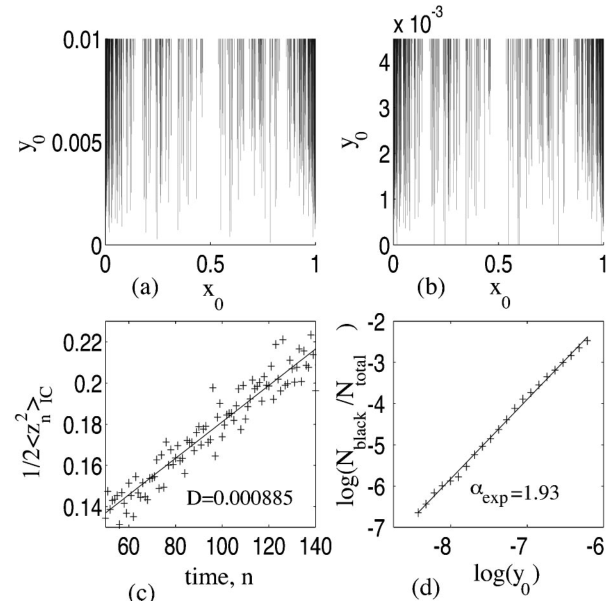


FIG. 4. (a), (b) Basins of attraction for Eqs. (12) and (13) for $\epsilon = 0.926$ and 0.928, respectively. To obtain (c) we uniformly sprinkle $L = 1.5 \times 10^6$ initial conditions in $y_0 = 0$, $0 < x_0 < 1$. We then iterate them 200 iterates and find that there are $l = 950$ orbits which still stay at a distance larger than 0.1 from the period-three attractor. Then we plot $1/2\langle z_n^2\rangle_{\text{IC}}$ versus $n$, where $\langle\cdots\rangle_{\text{IC}}$ denotes an average over the $l = 950$ orbits still not near the period-three attractor. The value of $D$ is then estimated as the slope of the straight line fit to the numerical data; (d) the fraction of initial conditions going to $y = \infty$ as a function of $y$. $\alpha_{\text{exp}}$ is obtained as the slope of the straight line fit to the data in a log–log scale. (c), (d) Correspond to the situation where $\epsilon = 0.926$.

To obtain the values of $\langle h_\perp\rangle$ for the chaotic transient set (the second column of Table I) we first uniformly sprinkle many initial conditions in $y_0 = 0$, $0 < x_0 < 1$. We then iterate these initial conditions $M$ iterates. At time $M \gg 1$ most of the sprinkled orbits will be close to the attractor (say within a distance of 0.1). However, if the number of sprinkled orbits is large, there will still be orbits that are not near the attractor. We make the number of initial conditions sprinkled large enough so that there are still many initial conditions not near the attractor at time $M$. We then approximate $\langle h_\perp\rangle$ by

$$\langle h_\perp\rangle \cong \left\langle \frac{1}{M}\sum_{n=1}^{M} |\ln N_{1y}(x_n,0)| \right\rangle_{\text{IC}},$$

where $N_{1y}(x,y) = \partial N_1/\partial y$ and $\langle\cdots\rangle_{\text{IC}}$ denotes an average over those initial conditions whose orbits are not near the attractor in $y=0$ at time $M$. The value of $D$ (the third column of Table I) was obtained by noting that the quantity

$$z_n = \sum_{m=1}^{n} (\ln|N_{1y}(x_m,0)| - \langle h_\perp\rangle)$$

TABLE I. Data for example 1.

| $\epsilon$ | $\langle h_\perp\rangle$ | $D$ | $\alpha_{\text{th}}$ | $\alpha_{\text{exp}}$ |
|---|---|---|---|---|
| 0.920 | 0.0164 | 0.000 920 | 2.49 | 2.14 |
| 0.923 | 0.0200 | 0.000 917 | 2.12 | 2.16 |
| 0.926 | 0.0233 | 0.000 885 | 1.87 | 1.93 |
| 0.928 | 0.0256 | 0.000 864 | 1.72 | 1.74 |

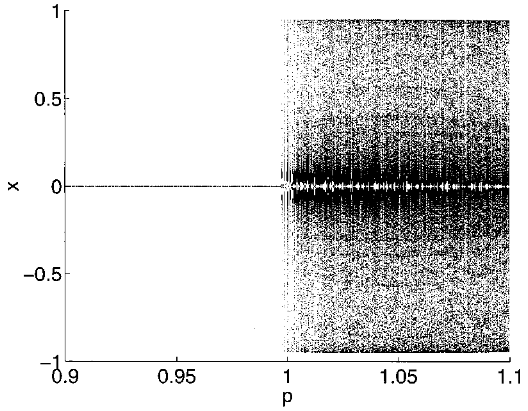


FIG. 5. Bifurcation diagram for Eq. (14).

undergoes unbiased diffusion while the orbit is in the chaotic transient. Thus we plot $\frac{1}{2}\langle z_n^2\rangle_{\rm IC}$ vs $n$, and estimate $D$ as the slope of a straight line fit to the data [see Fig. 4(c) for an example of such a plot]. The fourth column of Table I. $\alpha_{\rm th}$, is then given by inserting $\langle h_\perp\rangle$ and $D$, as found above, into Eq. (10). The value of the experimental exponent $\alpha_{\rm exp}$ (the fifth column of Table I) was obtained by estimating the fraction of ''black'' dots in the basin of attraction (those that lead to $y\to\infty$) as a function of $y$, and plotting this fraction as a function of $y$ using a log–log scale. We find that, for sufficiently small $y$, such plots are, in accord with the predicted $y^\alpha$ dependence, well-fit by a straight line [see Fig. 4(d), for example]. The slope of such a fit gives $\alpha_{\rm exp}$. One can see from Table I that $\alpha_{\rm exp}$ agrees reasonably well with its predicted value $\alpha_{\rm th}$.

*Example 2*: We consider the two-dimensional map,

$$x_{n+1}=M_2(x_n,r)=x_n[r(12.3-7r)x_n^4-r(11.3-7r)x_n^2+x_n^2-r], \tag{14}$$

$$y_{n+1}=N_2(x_n,y_n,\epsilon,\epsilon')=\{1+\epsilon-\epsilon'[1+\cos(\pi x_n)]\}y_n+y_n^3. \tag{15}$$

TABLE II. Data for example 2.

| $\epsilon$ | $\langle h_\perp\rangle$ | $D$ | $\alpha_{\rm th}$ | $\alpha_{\rm exp}$ |
|---|---|---|---|---|
| 0.150 | 0.005 | 0.011 | 1.59 | 1.62 |
| 0.155 | 0.010 | 0.011 | 1.40 | 1.42 |

This system has the same general properties as in the map of the previous example. However, $M_2(x_n,r)$, the map in the invariant manifold, is an example[11] exhibiting type-iii intermittency.[10] The bifurcation diagram for $M_2(\cdot)$ is shown in Fig. 5. This map has a period-one orbit at $x=0$. As the parameter $r$ increases through $r_c=1$, this period-one orbit becomes unstable, experiencing an inverse period doubling bifurcation. The map has a chaotic attractor for $r>1$. The parameter $r$ was taken to be equal to 0.95; $M_2(\cdot)$ is contracting at the fixed point $x=0$ and repelling on a transient. For this value of $r$, we obtain $\tau=28.0$. The basin of attraction is shown in Fig. 6. Table II gives the values of $\langle h_\perp\rangle$, $D$, $\alpha_{\rm th}$, and $\alpha_{\rm exp}$ for $\epsilon'=0.1$, and two different values of the other normal parameter $\epsilon$.

*Example 3*: The third system we studied is a modification of a flow that describes the motion of a particle in a two-dimensional $(x,y)$ double potential well[3] $V(\mathbf{r})=(1-x^2)^2+(x+\overline{x})y^2$. The particle is a subject to friction and time harmonic forcing,

$$d^2\mathbf{r}/dt^2=-\gamma d\mathbf{r}/dt-\nabla V(\mathbf{r})+f_0\sin(\omega t)\hat{\mathbf{x}}. \tag{16}$$

Here $\hat{\mathbf{x}}$ is the unit vector in the $x$ direction and $\gamma$, $f_0$, $\omega$, and $\overline{x}$ are parameters. For appropriate $(\gamma,f_0,\omega,\overline{x})$ this system is known to exhibit a riddled basin.[3] The phase space of this problem is five dimensional with coordinates $x$, $dx/dt$, $y$, $dy/dt$, and $\theta=(\omega t) \bmod 2\pi$. From the symmetry of the potential the problem is invariant with respect to $y\to -y$, and, therefore, $y=dy/dt=0$ specifies a three-dimensional invariant hyperplane in the full five-dimensional phase space. The dynamics in this invariant hyperplane is obtained by setting $y$ and $dy/dt$ equal to zero in Eq. (16). This yields

$$d^2x/dt^2+\gamma\, dx/dt-4x(1-x^2)=f_0\sin(\omega t). \tag{17}$$

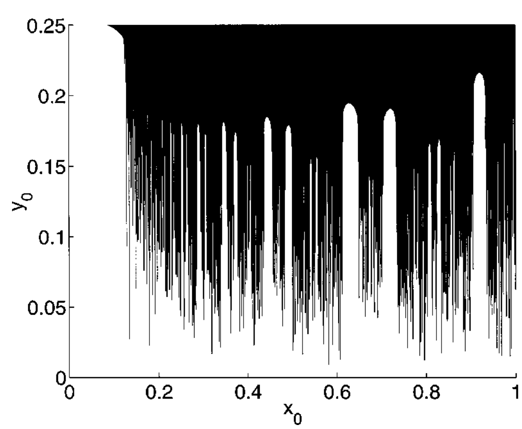


FIG. 6. Basin of attraction for Eqs. (14) and (15) obtained on a 2000 $\times$2000 grid of initial conditions. $r=0.95$, $\epsilon=0.135$, $\epsilon'=0.1$.

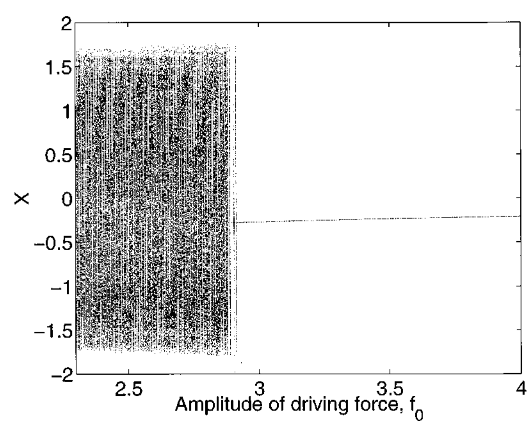


FIG. 7. Bifurcation diagram for Eq. (17).

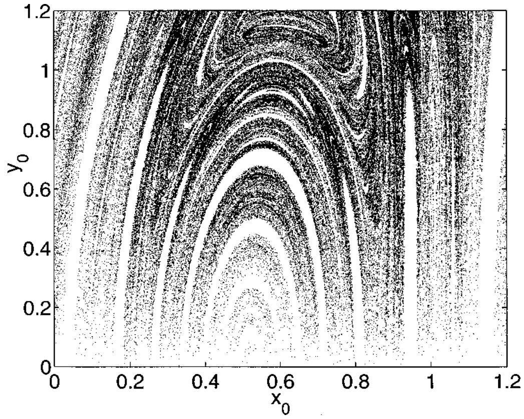


FIG. 8. Numerical basin for Eq. (16) obtained on $1000\times1000$ initial conditions. Following Ref. 4 we iterate each initial condition forward in time until the trajectory either gets very close to the invariant plane $y=0$ ($|y|<10^{-8}$, $|v_y|<10^{-9}$, and $yv_y<0$), or else is definitely in the repelling region ($|y|>20$, $|v_y|>100$, and $yv_y>0$). Closed circles correspond to initial conditions eventually attracted to $\infty$.

We analyzed Eq. (16) in terms of a stroboscopic Poincaré section corresponding to the period of the forcing, i.e., we consider the times $\omega t \bmod 2\pi=0$. This lead to a four-dimensional discrete-time mapping.

In previous work using model (16), the parameters $\gamma$, $f_0$, and $\omega$ were chosen so that Eq. (17) had a chaotic attractor. In this case, appropriate choice of the parameter $\overline{x}$ yields basin riddling for the $y=0$ attractor. Here we consider a modification of Eq. (16) such that the dynamics in $y=0$ is such that the attractor is periodic, but there is also a chaotic transient. In particular, we replace $\overline{x}$ by a time periodic quantity $\overline{x}=\overline{x}_0+\overline{x}_1\sin(\omega t-\phi)$ and set the parameters at $\overline{x}_0=4.4$, $\overline{x}_1=2.9$, $\phi=0.15$, $\gamma=0.05$, and $\omega=3.5$. Varying the remaining parameter $f_0$ we obtain a bifurcation diagram for Eq. (17) (see Fig. 7). As $f_0$ is decreased there is a type-iii intermittency transition to chaos [similar to the map (15)]. For $f_0=4.0$ the average lifetime of a chaotic transient is $\tau=12.0$. In order to estimate $\langle h_\perp\rangle$ we integrated the equations for the tangent vector representing the infinitesimal variations from the invariant plane $y=v_y=0$: $d\delta y/dt=-\gamma\delta v_y-2(x+\overline{x})\delta y$, $d\delta y/dt=\delta v_y$, where $\delta y$ and $\delta v_y$ are infinitesimal variations (Fig. 8). The results are presented in Table III and we again find reasonably good agreement between our estimates of $\alpha_{\text{th}}$ and $\alpha_{\text{exp}}$.

## V. CONCLUSION

In this paper we have considered systems with an invariant manifold in which are located both a nonattracting chaotic set and a nonchaotic attractor (e.g., a periodic orbit). Thus, in this situation, typical initial conditions in the invariant manifold may yield orbits that experience chaotic transients before approaching the chaotic attractor. It is found that the basin boundary separating the basins of the attractor in the invariant manifold and another attractor not in the invariant manifold is characterized by stalactitelike structure, thin cusp-shaped regions extending down to touch the invariant manifold at the location of points in the nonattracting chaotic set. Using a random walk model, we have obtained a scaling relation for the variation of the measure of the basin of the attractor not in the invariant manifold. In particular, we show that this basin's measure in a surface at a small distance $y$ from the invariant manifold scales as a power law $y^\alpha$, and we have obtained a theoretical prediction for the scaling exponent $\alpha$. This prediction has been tested with good results by comparison with various numerical experiments.

TABLE III. Data for example 3.

| $\langle h_\perp\rangle$ | $D$ | $\alpha_{\text{th}}$ | $\alpha_{\text{exp}}$ |
|---|---|---|---|
| 0.030 | 0.0285 | 1.26 | 1.29 |


## ACKNOWLEDGMENT

The work was supported by the Office of Naval Research (Physics).


## APPENDIX: DERIVATION OF EQ. (10)

The solution to Eq. (7) subject to the boundary condition $\overline{P}(0,\overline{y}_1,s)=0$ is

$$\overline{P}(\overline{y},\overline{y}_1,s)=\begin{cases} A(\exp[\kappa_a\overline{y}]-\exp[\kappa_b\overline{y}]), & 0<\overline{y}<\overline{y}_1 \\ B\exp[-\kappa_a\overline{y}] & \overline{y}>\overline{y}_1, \end{cases} \tag{A1}$$

where

$$\kappa_a=\frac{1}{2D}\left(\sqrt{\langle h_\perp\rangle^2+4D(s+1/\tau)}+\langle h_\perp\rangle\right),$$

$$\kappa_b=\frac{1}{2D}\left(\sqrt{\langle h_\perp\rangle^2+4D(s+1/\tau)}-\langle h_\perp\rangle\right),$$

$$A=-\frac{\exp[-\kappa_b\overline{y}_1]}{(\kappa_a+\kappa_b)D},$$

$$B=-\frac{\exp[-\kappa_b\overline{y}_1]-\exp[\kappa_a\overline{y}_1]}{(\kappa_a+\kappa_b)D}.$$

Thus

$$\begin{aligned}\int_0^\infty\overline{P}(\overline{y},\overline{y}_1,s)\,d\overline{y}&=\int_0^{\overline{y}_1}\overline{P}\,d\overline{y}+\int_{\overline{y}_1}^\infty\overline{P}\,d\overline{y}\\ &=A[(1-\exp[-\kappa_a\overline{y}_1])/\\ &\quad\kappa_a-(\exp[\kappa_b\overline{y}_1]-1)/\kappa_b]\\ &\quad+B\exp[-\kappa_a\overline{y}_1])/\kappa_a\\ &=\frac{1-\exp[-\kappa_b\overline{y}_1]}{s+1/\tau}.\end{aligned}$$

Finally,

$$P_{y=0}=\frac{1}{\tau}\int_0^\infty\int_0^\infty P(\overline{y},\overline{y_1},n)\,d\overline{y}\,dn$$

$$=\frac{1}{\tau}\int_0^\infty \overline{P}(\overline{y},\overline{y_1},0)\,d\overline{y}$$

$$=1-\exp[-\alpha\overline{y_1}]=1-y_1^{\alpha},$$

where $\alpha$ is $\kappa_b$ with $s$ set equal to zero. Thus

$$P_\infty=1-P_{y=0}=y_1^{\alpha},$$

which is Eq. (10).


[1] J. Milnor, Commun. Math. Phys. **99**, 177 (1985).

[2] J. C. Alexander, I. Kan, J. A. Yorke, and Z. You, Int. J. Bifurcation Chaos Appl. Sci. Eng. **2**, 795 (1992).

[3] J. C. Sommerer and E. Ott, Nature (London) **365**, 136 (1993).

[4] E. Ott, J. C. Alexander, I. Kan, J. C. Sommerer, and J. A. Yorke, Physica D **76**, 384 (1994); Phys. Rev. Lett. **71**, 4134 (1993).

[5] Diffusion models have also been used in the related problem of on–off intermittency. For example, see T. Yamada and H. Fujisaka, Prog. Theor. Phys. **76**, 582 (1986); H. Hata and S. Miyazaki, Phys. Rev. E **55**, 5311 (1997).

[6] P. Ashwin, J. Buescu, and I. N. Stewart, Phys. Lett. A **193**, 126 (1994); Nonlinearity **9**, 703 (1996).

[7] P. Ashwin, E. Covas, and R. Tavakol, Nonlinearity **12**, 563 (1999).

[8] S. C. Venkataramani, B. Hunt, and E. Ott, Phys. Rev. E **54**, 1346 (1996).

[9] S. W. McDonald, C. Grebogi, E. Ott, and J. A. Yorke, Physica D **17**, 125 (1985).

[10] Y. Pomeau and P. Manneville, Commun. Math. Phys. **74**, 189 (1985).

[11] W. Yang, M. Ding, A. J. Mandell, and E. Ott, Phys. Rev. E **51**, 102 (1995).

[12] Y. C. Lai and C. Grebogi, Phys. Rev. Lett. **83**, 2926 (1999).